S-scheme heterojunction photocatalyst P25/CuI

M. Nadareishvili[1*], T. Zedginidze[1], A. Kurtanidze[1], M. Mdzinarashvili[2], J. Ramsden[3]
[1]Department of Condensed Matter Physics, E.Andronikashvili Institute of Physics, Ivane, Javakhishvili Tbilisi State University, Georgia; malkhaz.nadareishvili@tsu.ge (M.N.).
[2]Department of Physics, Ivane Javakhishvili Tbilisi State University, Georgia.
[3]University of Buckingham, United Kingdom.

Abstract: The S-Scheme photocatalyst P25/CuI was developed based on the commercial photocatalyst P25. Comparative studies were conducted to examine the properties of this photocatalyst, as well as cluster-free P25 and P25/Co, which is decorated with metal clusters. The structural features of these materials were analyzed using X-ray diffraction (XRD) and energy-dispersive X-ray spectroscopy (EDS). It was found that the starting material P25 consisted of a mixture of two modifications of titanium dioxide (TiO2): anatase and rutile, with a content of 87.6% and 12.4%, respectively. The electron paramagnetic resonance (EPR) spectra of these substances were also studied, and their distinctive features were identified. Additionally, the changes in the energy band gap of P25 upon the deposition of Co and CuI clusters were determined through optical scattering spectra. It was found that while the well in the scattering spectrum reflecting the gap in the energy spectrum of P25 changes insignificantly upon the deposition of cobalt (Co) clusters, upon the deposition of copper iodide (CuI) clusters, an additional well appears in the long-wavelength region, which leads to an increase in the sensitivity of the catalyst to visible light. The optical absorption spectra indicated a significant reduction in photoinduced charge recombination in the S-Scheme P25/CuI compared to conventional photocatalysts that are decorated with metal cocatalysts. The comparative efficiency of the considered photocatalysts was studied using a methylene blue solution.

Keywords: Decoration of clasters, EPR and optical study of photocatalystsP25 photocatalist, Photocatalysts, cocatalysts.

1. Introduction

Photocatalysis refers to the activation of oxidation-reduction reactions in the environment through the influence of light rays. This reaction holds promising potential in various applications. In particular, photocatalysis can decompose water into oxygen and hydrogen and can serve as an environmentally friendly fuel [1]. Additionally, it can break down harmful substances and bacteria in the environment, highlighting its ecological benefits [2-5]. To facilitate photocatalysis, specific substances known as photocatalysts are required to carry out the photocatalysis reaction. These photocatalysts are semiconductor substances that generate electrons and holes when exposed to light. Once created, these charges move to the surface, where they interact with environmental molecules and initiate their decomposition. Since the reaction occurs at the surface, photocatalysts are typically used in the form of nanopowders, thin films or other nanoforms, which help maximize surface area for more efficient reactions [6-10].

The main obstacle preventing the widespread practical application of photocatalysis is the insufficient efficiency of the reaction. This inefficiency is primarily due to photoinduced charge recombination and the use of ultraviolet rays mainly by natural photocatalysts, which make up only a small portion of solar radiation [11]. Moreover, these natural photocatalysts have a large energy gap, while those with a smaller band gap lack the necessary boundary potentials in their valence and conduction bands to split

water molecules [12]. Consequently, a key challenge in the field of photocatalysis is to develop methods to enhance efficiency and to create new more effective photocatalysts.

To reduce charge recombination, researchers use cocatalysts, which are small clusters deposited on the surface of photocatalysts [13]. For years, metal clusters have served as cocatalysts (see Figure 1a) [14] because they capture electrons and prevent recombination. However, in recent years, semiconductor cocatalysts have gained popularity. In these systems, recombination occurs between electrons in the conduction band of the photocatalyst and holes in the valence band of the cocatalyst. This process leads to an accumulation of induced holes in the valence band of the photocatalyst and induced electrons in the conduction band of the cocatalyst (see Figure 1b) [15]. Photocatalysts utilizing this mechanism are referred to as S-Scheme heterojunction photocatalysts [16].
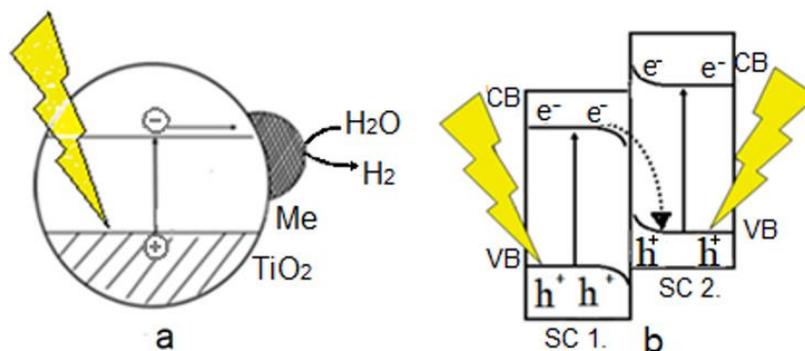

Figure 1.
a) photocatalyst with a metal cocatalyst, b) S-Scheme photocatalyst.

To improve the efficiency of visible light in the photocatalysis process, various methods are employed to modify the energy bandgap, for example the introduction of impurities, vacancies etc [17-21].

Currently available photocatalysts are characterized by a variety of properties: some are more effective, some are less effective, some contain harmful substances, some do not, some are expensive, some are cheap, some are available in small quantities and cannot meet the needs of the Earth's population, etc. Therefore, a photocatalyst cannot be estimated only by its efficiency. For the studies we selected P25, which is characterized by average efficiency, but has such excellent other properties that it is considered as one of the most promising materials for photocatalyst. The aim of the studies was to determine whether it is possible to increase its efficiency by using one specific S-scheme cocatalyst method. Obviously, to achieve maximum efficiency, other methods need to be used in conjunction with it.

2. Materials and Technology

This paper discusses the development of the S-Scheme photocatalyst P25/CuI, which was produced as a result of our studies, along with an examination of its properties. The starting material for these studies was P25, the mixture of the modification of the titanium dioxide (TiO_2). It is important to note that TiO_2 exists in several modifications; in this case, we chose a mixture of anatase and rutile known as P25 Degussa, which is recognized for its superior activity compared to the individual forms. The nano powders used in this research were purchased from Sigma Aldrich, boasting a purity of 99.5%. This said substance was selected due to its many advantageous properties, including non-toxicity, chemical resistance, low photo-corrosion, relatively high photocatalytic activity, a small energy gap, suitable conduction and valence band potentials that align with the dissociation potential of water molecules, its cost-effectiveness, etc. The cocatalyst substance CuI was also purchased from Sigma Aldrich, with a purity of 99%. This substance was selected because it shares similar beneficial properties with TiO_2, and

at the same time, its energy levels are appropriately aligned with those of TiO_2, as illustrated in Figure 1 b.

The preparation of P25/CuI photocatalytic nanocomplexes was based on a non-electrical chemical nanotechnology for decorating nanopowders, which was developed in our laboratory [22, 23]. However, at the same time, it was necessary to modify this process slightly for the said substances. The final procedure is as follows: weigh 0.5 g of P25 Degussa, add 40 ml of distilled water to the powder; for complete mixing, the suspension should be placed in an ultrasonic device and stirred for 20 min, resulting in a slightly thick, homogeneous suspension

In parallel, 0.5 g of CuI powder should be weighed and dissolved in 30 mL of acetonitrile while stirring constantly for 15 min. Next, the solution should be placed in a separatory funnel and added dropwise to the Degussa suspension, which is heated to 80° C, while maintaining constant stirring. After the CuI solution has been completely added, the suspension should continue to be stirred until the solvent, acetonitrile, has evaporated fully.

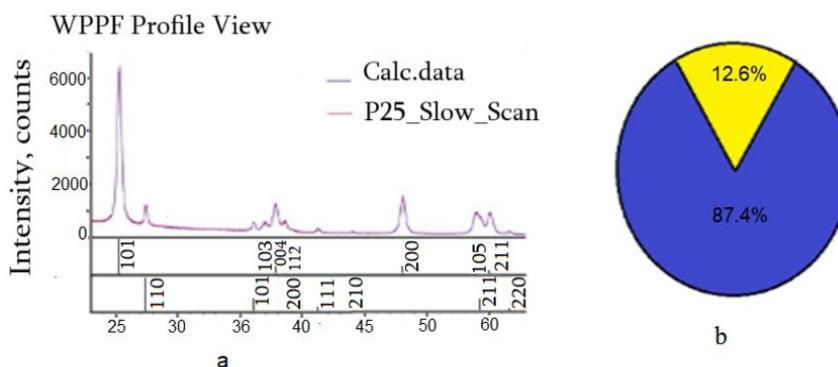The resulting suspension should then be washed 4 to 5 times using a centrifuge and dried in a drying cabinet at 70°C.

Figure 2.
a) XRD results of the p25, b) Phase composition of the p25.

3. Results and Discussion

X-ray diffraction (XRD) and energy dispersive spectroscopy (EDS) studies of the purchased P25 powders were conducted, and the results are shown in Figure 2. Figure 2a presents the results from the XRD (X-ray diffraction) studies. Analysis was performed to determine the phase composition of the sample, revealing the presence of both anatase and rutile phases. The XRD pattern revealed the presence of both anatase and rutile phases in the sample. The anatase phase was identified as the dominant phase, with diffraction peaks observed at 25.2°, 37.7°, 48.0°, 53.8°, and 55.0°, corresponding to the (101), (004), (200), (105), and (211) planes, respectively. In contrast, the rutile phase was present in a minor amount, displaying peaks at 27.4°, 36.0°, 41.2°, 44.0°, and 56.6°, which correspond to the (110), (101), (111), (210), and (220) planes. In conclusion, the XRD analysis indicates that the sample primarily consists of the anatase phase, with a minor contribution from the rutile phase. The anatase content was found to be 87.4%, while the rutile content was 12.6% (Figure 2b).

Figure 3 shows the results of EDS studies conducted after the deposition of CuI clusters on P25, which reflects the elemental composition of P25/CuI.
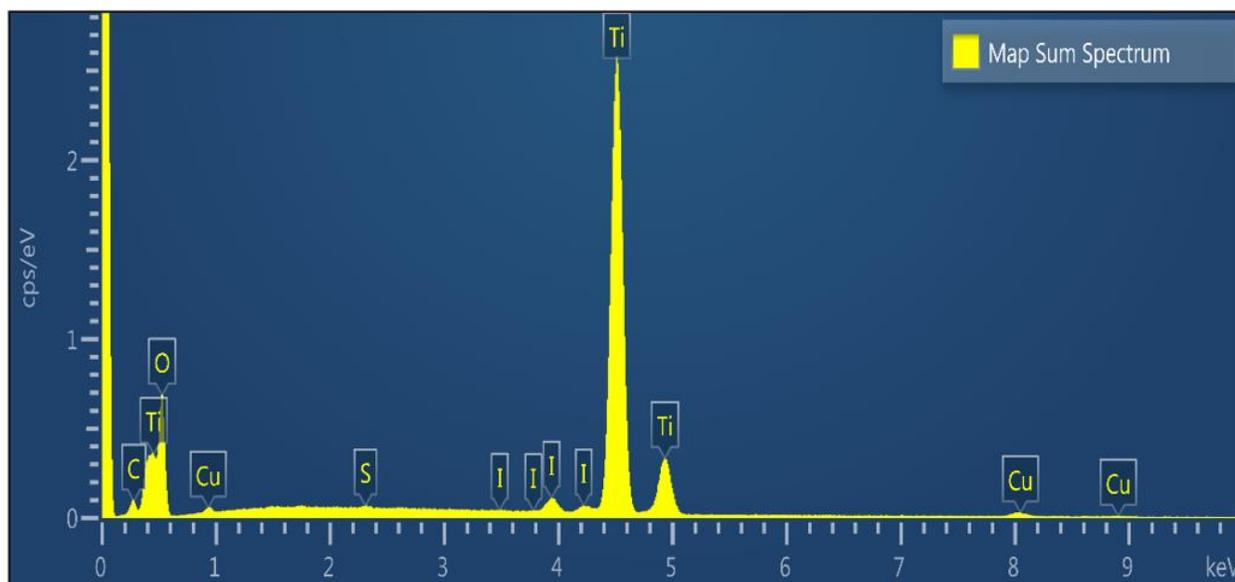
Figure 3.
EDS speqtrum of the P25/CuI.

EDS studies show that the test sample P25/CuI contains 6 elements: Titanium, Oxygen, Copper, Iodine, Carbon and Sulfur.
Table 1 shows the quantitative content of these elements in the photocatalyst.

Table 1.
Elemental composition of P25 after decoration with CuI clusters.

Element	Line Type	Weight %	Weight % Sigma	Atomic %
Ti	K series	47.02	0.29	23.68
O	K series	44.97	0.33	67.82
I	L series	2.81	0.09	0.53
Cu	K series	1.45	0.08	0.55
C	K series	3.65	0.15	7.34
S	K series	0.10	0.02	0.07
Total		100.00		100.00

EDS studies conducted following the deposition of CuI clusters indicates that the amount of CuI relative to P25 Degussa is approximately 4.3 weight% and the total amount of other impurities does not exceed 3.8 weight% (Table I).

Figure 4 illustrates the results of the electron paramagnetic resonance (EPR) studies. Figure 4a shows the EPR spectrum of the P25 sample before the deposition of any cocatalysts. Figure 4b displays the EPR spectrum after the deposition of the nickel (Ni) cocatalyst on the surface of the P25 nanoparticles, while Figure 4c shows the EPR spectrum after the deposition of the CuI cocatalyst.
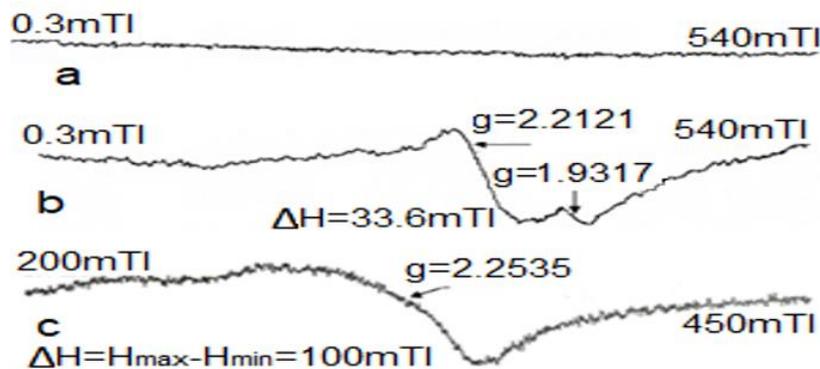
Figure 4.
 a) EPR spectrum of P25, b) EPR spectrum of P25/Ni photocatalyst, c) EPR spectrum of P25/CuI S-Scheme photocatalyst.

These studies demonstrate that the P25 material does not exhibit an Electron Paramagnetic Resonance (EPR) spectrum. However, EPR signals emerge after the deposition of cocatalyst clusters. Specifically, two signals appear with factors g=2.2121 and g=1.9317 following the deposition of nickel (Ni), while a signal with factor g=2.2535 appears after the deposition of copper(I) iodide (CuI). These findings suggest that the decoration of nanoparticles with cocatalysts does not simply deposit these clusters on the surface of nanoparticles, but rather involves the formation of strong chemical bonds between the atoms of these substances, leading to the generation of EPR signals.

Figure 5 illustrates the optical scattering spectra of the said samples within the wavelength range of 240 nm to 800 nm. Curve 1 in Figure 5 displays the scattering spectrum of P25 before cluster deposition. Curve 2 corresponds to the scattering spectrum of P25 after the deposition of Ni clusters, while Curve 3 represents the scattering spectrum of P25 after CuI cluster deposition.

The data indicate that after depositing Ni clusters, the well in the P25 spectrum associated with the gap in the energy spectrum of the semiconductor slightly broadens. In contrast, the deposition of CuI clusters introduces a second well in the visible region of the scattering spectrum, indicating an enhancement in light absorption in the visible region. This secondary well can be attributed to the energy gap CuI. Therefore, the addition of CuI clusters significantly improves the visible light absorption properties of P25
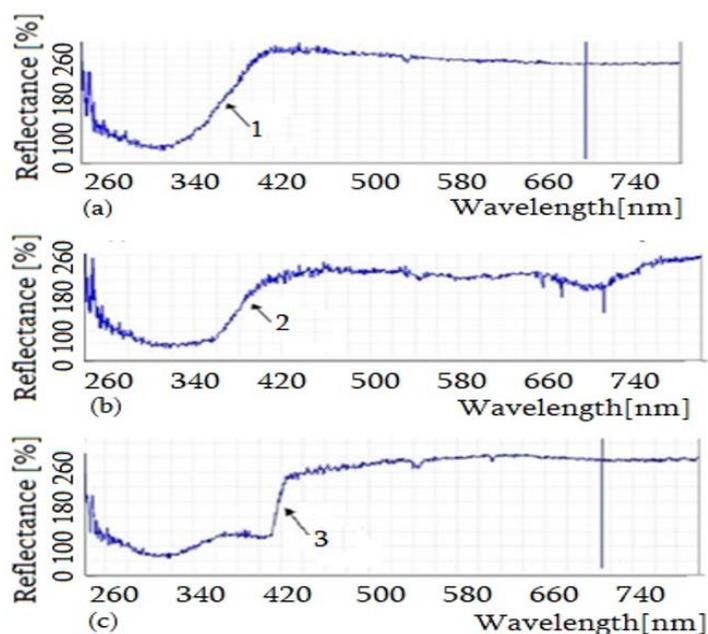
Figure 5.
Optical scattering spectra.

1) Optical scattering spectrum of P25, 2) Optical scattering spectrum of P25/Ni, 3) Optical scattering spectrum of P25/CuI

To assess whether photoinduced charge recombination is reduced, it is essential to examine the absorption spectra of the photocatalysts. Figure 6 displays the optical absorption spectra of the substances studied over a wavelength range of 185 nm to 800 nm.
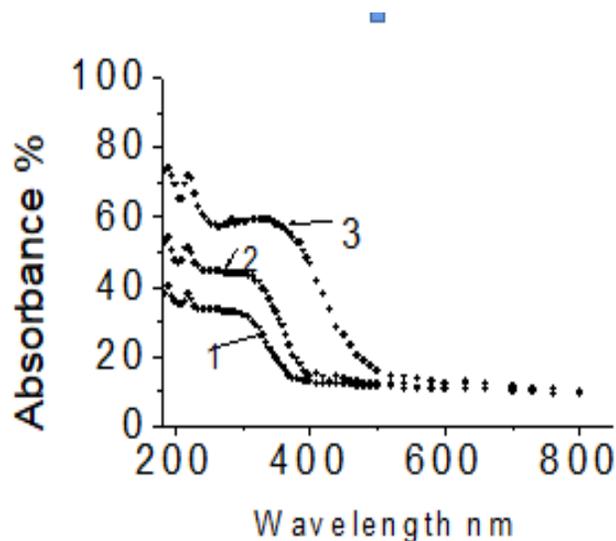
Figure 6.
Optical absorption spectra.

1) absorption spectrum of P25, 2) absorption spectrum of P25/Ni, 3) absorption spectrum of P25/CuI

Curves 1, 2, and 3 on figure 6 correspond to the optical absorption spectra of P25, P25/Ni, and P25/CuI, respectively. Curve 1 exhibits two peaks in the shorter wavelength range at approximately 190 nm and 220 nm. This occurs because P25 is a mixture of two titanium dioxide modifications: anatase and rutile, which possess slightly different energy bandgaps. Figure 7 presents a magnified view of these peaks.
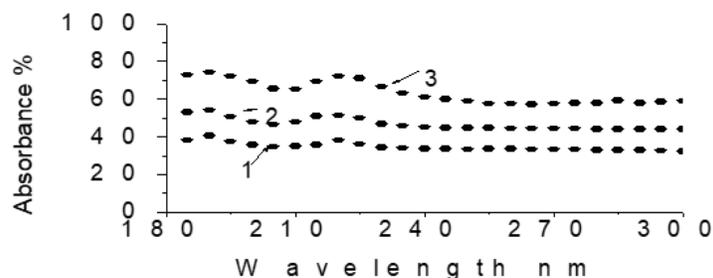

Figure 7.
1) Absorption curve of P25, 2) Absorption curve of P25/Ni, 3) Absorption curve of P25/CuI

The peak at 190 nm in Figure 7 corresponds to the rutile modification, while the peak at 220 nm corresponds to the anatase modification, which is validated by the spectra of pure anatase and rutile that we recorded. Curve 2 also displays these two peaks, while Curve 3, in addition to these two peaks, shows a third peak at approximately 325 nm. This third peak can be attributed to the energy gap in the spectrum of CuI. Regarding photoinduced charge recombination, the data indicates that light absorption increases with the deposition of Co clusters, suggesting a decrease in charge recombination. This reduction should enhance the efficiency of the photocatalyst. For P25/CuI, the increase in light absorption is even more pronounced. Therefore, we can infer that charge recombination is minimal for this sample, leading to its maximal efficiency.

To evaluate the actual efficiency of the photocatalysts being studied, we used a methylene blue solution. Figure 8 displays the decomposition curves for methylene blue corresponding to the photocatalysts we prepared.
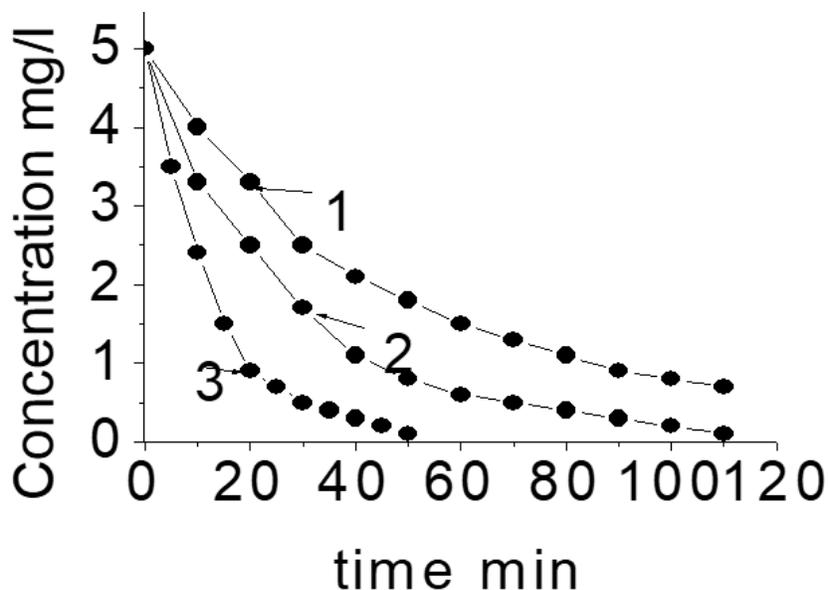
Figure 8.
1) Methylene decomposition curve by P25, 2) Methylene decomposition curve by
P25/Ni, 3) Methylene decomposition curve by P25/CuI.

The efficiency of each photocatalyst was assessed by monitoring the rate of methylene decomposition in a suspension containing both the methylene solution and the photocatalyst powder when exposed to light [24]. This decomposition rate was determined by measuring the change in methylene concentration over time. The methylene concentration was quantified by analyzing the absorption peak at a wavelength of 650 nm using a spectrophotometer, which had been previously calibrated with solutions of known methylene concentrations. Curves 1, 2, and 3 (Figure 8) represent the time-dependent methylene decomposition rates for P25, P25/Ni, and P25/CuI, respectively. The graphs indicate that the efficiency of the commercial P25 photocatalyst increases with the deposition of Ni clusters; however, the efficiency increases even more significantly with the deposition of CuI clusters. Specifically, the efficiency increases when incorporating CuI is nearly double that observed with Ni. This enhanced performance is attributed to both a reduction in the recombination of photoinduced charges and a more complete utilization of visible light energy. The initial concentration of the methylene solution was 5 mg/L, and sunlight was used as the light source.

4. Conclusions

The research focuses on titanium dioxide nanopowders, specifically P25, which is a mixture of two modifications: anatase and rutile. P25 is characterized for its higher photocatalytic efficiency compared to each modification when assessed individually. A novel method for depositing copper iodide (CuI) clusters on P25 was developed, leading to the synthesis of a new S-Scheme photocatalyst, P25/CuI. X-ray diffraction (XRD) and energy-dispersive spectroscopy (EDS) studies revealed that this photocatalyst maintains both modifications, with a composition of 87.4% anatase and 12.6% rutile. We conducted comparative studies on the S-Scheme photocatalyst P25/CuI, nickel-decorated P25 (P25/Ni), and pure P25, exposing the peculiarities characteristics of P25/CuI. Electron paramagnetic resonance (EPR) studies revealed that P25/CuI exhibits a distinct EPR signal, with a g factor of 2.2535. Additionally, optical scattering spectra indicated that the well observed in the scattering spectrum of P25, which is associated to the band gap in its energy spectrum, shows only a minor change when Ni clusters are deposited, indicating small changes in its sensitivity to visible light. Upon the deposition of CuI clusters, a second well appears in the visible region, which is associated with the band gap in the CuI energy

spectrum. This suggests that the sensitivity of this photocatalyst to visible light has increased. Consequently, an additional absorption peak in the visible region was observed in the optical absorption spectra of P25/CuI. Furthermore, there was an overall increase in absorption across the optical absorption spectra, indicating a decrease in photoinduced charge recombination in the S-Scheme photocatalyst. This decrease is a crucial factor in increasing photocatalytic efficiency. In fact, when studying the photocatalytic efficiency of the said substances using a methylene blue solution, it was demonstrated that the S-Scheme photocatalyst's efficiency exceeds the result achieved when using a conventional, non-noble metal cluster-decorated photocatalyst by about 200%.

Thus, the conducted studies showed that P25, in addition to the previously known positive photocatalytic properties, is characterized by a significant increase in efficiency when using S-scheme cocatalysts. Therefore, it is necessary to continue research on P25 with the complex use of other S-scheme cocatalysts and methods for increasing sensitivity to visible light to achieve maximum efficiency.

Funding:

Transparency:

The authors confirm that the manuscript is an honest, accurate, and transparent account of the study; that no vital features of the study have been omitted; and that any discrepancies from the study as planned have been explained. This study followed all ethical practices during writing.

Copyright:

References

[1] N. Fajrina and M. Tahir, "A critical review in strategies to improve photocatalytic water splitting towards hydrogen production," *International Journal of Hydrogen Energy*, vol. 44, no. 2, pp. 540-577, 2019.

[2] A. Clemente *et al.*, "Staphylococcus aureus resists UVA at low irradiance but succumbs in the presence of TiO2 photocatalytic coatings," *Journal of Photochemistry and Photobiology B: Biology*, vol. 193, pp. 131-139, 2019. https://doi.org/10.1016/j.jphotobiol.2019.02.009

[3] V. Amrute, K. Supin, M. Vasundhara, and A. Chanda, "Observation of excellent photocatalytic and antibacterial activity of Ag doped ZnO nanoparticles," *RSC Advances*, vol. 14, no. 45, pp. 32786-32801, 2024. https://doi.org/10.1039/D4RA05197A

[4] L. Predoană *et al.*, "Photocatalytic performance of Sn–doped TiO2 nanopowders for photocatalytic degradation of methyl orange dye," *Catalysts*, vol. 13, no. 3, p. 534, 2023. https://doi.org/10.3390/catal13030534

[5] M. Nadareishvili, T. Gegechkori, G. Mamniashvili, T. Zedginidze, and T. Petriashvili, "Synergetic water purification modulus for the methylene degradation in the water-methylene mixtures," *Edelweiss Applied Science and Technology*, vol. 9, no. 2, pp. 266-275, 2025. https://doi.org/10.55214/25768484.v9i2.4464

[6] A. Mir, N. Becheikh, L. Khezami, M. Bououdina, and A. Ouderni, "Sinthesis, characterization, and study of the photocatalytic activity upon polimeric-surface modification of ZnO nanoparticles," *Engineering, Technology & Applied Science Research*, vol. 13, no. 6, pp. 12047-12053, 2023. https://doi.org/10.48084/etasr.6373

[7] S. A. Mousa, D. Wissa, H. Hassan, A. Ebnalwaled, and S. Khairy, "Enhanced photocatalytic activity of green synthesized zinc oxide nanoparticles using low-cost plant extracts," *Scientific Reports*, vol. 14, no. 1, p. 16713, 2024. https://doi.org/10.1038/s41598-024-66975-1

[8] S. Wei, L. Wang, J. Yue, R. Wu, Z. Fang, and Y. Xu, "Recent progress in polymer nanosheets for photocatalysis," *Journal of Materials Chemistry A*, vol. 11, no. 44, pp. 23720-23741, 2023. https://doi.org/10.1039/D3TA05435G

[9] K. Z. Bolaghi, C. Rodriguez-Seco, A. Yurtsever, and D. Ma, "Exploring the remarkably high photocatalytic efficiency of ultra-thin porous graphitic carbon nitride nanosheets," *Nanomaterials*, vol. 14, no. 1, p. 103, 2024.

[10] T. Gavasheli, G. Mamniashvili, M. Nadareishvili, and T. Zedginidze, "Electroless technology for production of cobalt magnetic and Photocatalytic nanopowders and nanowires," *TechConnect Briefs*, vol. 17, pp. 42-45, 2019.

[11]   T. Gegechkori, G. Mamniashvili, T. Gagnidze, M. Nadareishvili, and T. Zedginidze, "Photocatalytic and magnetic properties of the TiO2 micro- and nanopowders decorated by magnetic cocatalysts," *Engineering, Technology & Applied Science Research*, vol. 13, no. 5, pp. 11924-11931, 2023. https://doi.org/10.48084/etasr.6244

[12]   K. Soojin, H. Yoo, and J. H. Kim, "Recent advances in earth-abundant photocatalyst materials for solar H2 production," *Advanced Powder Technology*, vol. 31, no. 1, pp. 11-28, 2020. https://doi.org/10.1016/j.apt.2019.08.035

[13]   V. Soni *et al.*, "Advances and recent trends in cobalt-based cocatalysts for solar-to-fuel conversion," *Applied Materials Today*, vol. 24, p. 101074, 2021. https://doi.org/10.1016/j.apmt.2021.101074

[14]   M. Nadareishvili *et al.*, "Decoration of photocatalytic TiO2 particles by cobalt clusters," *Nanotechnology Perceptions*, vol. 16, no. 3, pp. 336-347, 2020. https://doi.org/10.4028/www.scientific.net/NP.16.336

[15]   Q. Xu, L. Zhang, B. Cheng, J. Fan, and J. Yu, "S-scheme heterojunction photocatalyst," *Chem*, vol. 6, no. 7, pp. 1543-1559, 2020. https://doi.org/10.1016/j.chempr.2020.06.010

[16]   M. Jafar, Mohammad "Principles, mechanism, and identification of S-scheme heterojunction for photocatalysis: A critical review," *Journal of the American Ceramic Society*, vol. 107, no. 9, pp. 5695-5719, 2024. https://doi.org/10.1111/jace.19920

[17]   J. Xiaohui, J.-F. Lu, Q. Wang, and D. Zhang, "Impurity doping approach on bandgap narrowing and improved photocatalysis of Ca2Bi2O5," *Powder Technology*, vol. 376, pp. 708-723, 2020. https://doi.org/10.1016/j.powtec.2020.08.029

[18]   A.-G. Schiopu *et al.*, "Characterization of pure and Doped ZnO nanostructured powders elaborated in solar reactor," *Engineering, Technology & Applied Science Research*, vol. 14, no. 2, pp. 13502-13510, 2024. https://doi.org/10.48084/etasr.6923

[19]   M. Nadareishvili, Z. Tinatin, G. Salome, K. Ana, A. Meri, and R. Jeremy, "Influence of the surface conditions on the properties of the oxide photocatalysts," *European science review*, no. 5-6, pp. 8-12, 2023. https://doi.org/10.29013/ESR-23-5.6-8-12

[20]   Z. Wei, J. Liu, and W. Shangguan, "Defects engineering in photocatalytic water splitting materials," *ChemCatChem*, vol. 11, no. 24, pp. 6177-6189, 2019. https://doi.org/10.1002/cctc.201901579

[21]   N. Mediouni *et al.*, "Impact of structural defects on the photocatalytic properties of ZnO," *Journal of Hazardous Materials Advances*, vol. 6, p. 100081, 2022. https://doi.org/10.1016/j.hazadv.2022.100081

[22]   T. N. Khoperia, T. Zedginidze, K. Kvavadze, and M. Nadareishvili, "Development of competitive nanotechnologies for solution of challenges in photocatalysis, electronics and composites fabrication," in *ECS Meeting Abstracts*, 2007, no. 2: IOP Publishing, p. 107.

[23]   N. Malkhaz, K. Evgeni, S. Viktor, T. Genadi, and T. Severian, "New method of differential calorimetry," *European Science Review*, vol. 1-2, pp. 253-255, 2017.

[24]   M. Nadareishvili, "Impact of complex processing on the photocatalytic properties of titanium dioxide," *European Science Review*, vol. 9-10, pp. 2-6, 2021. https://doi.org/10.29013/ESR-21-9.10